Available online at www.sciencedirect.com
SCIENCE DIRECT®
Thermochimica Acta 421 (2004) 203–209
thermochimica acta
www.elsevier.com/locate/tca

Reversible melting of gel-spun fibers of polyethylene☆

Jeongihm Pak[a,b], Bernhard Wunderlich[a,b,*]

[a] *Department of Chemistry, The University of Tennessee, Knoxville, TN 37996-1600, USA*
[b] *Chemical Sciences Division, Oak Ridge National Laboratory, Oak Ridge, TN 37831-6197, USA*

Received 25 February 2004; received in revised form 20 March 2004; accepted 5 April 2004
Available online 28 May 2004

Abstract

The melting and crystallization of gel-spun, ultrahigh molar mass polyethylene (UHMM-PE) fiber is analyzed with both, standard differential scanning calorimetry (DSC) and temperature-modulated DSC (TMDSC) to identify the differences to extended-chain crystals of polyethylene. The analyzed samples were studied before with respect to their molecular mobility, morphology, and crystal and phase structure. The UHMM-PE contains a mobile, oriented mesophase and only few folded chains. The truly amorphous fraction is about 3%. Reversing melting and crystallization is observed for these fibers. It increases in amount on recrystallization after melting. Difficulties in measuring the original fibers arose from the shrinkage of the fibers and a resulting deformation of the sample pan. The new data are compared to literature information on other polyethylenes and linked to reversible melting of decoupled segments of the polymer chains contained in small, nanometer-size phases within the crystalline phase and the oriented-intermediate fractions.

Keywords: TMDSC; Melting; Crystallization; UHMM-PE; Fiber; Instrument lag; Decoupling

1. Introduction

A large number of studies by temperature-modulated differential scanning calorimetry, TMDSC, of reversing and reversible melting of different oligomer and polymer samples have been reviewed recently [1]. In this discussion of the degree of reversibility, the term *reversing* is used, as before, to characterize the response to the temperature modulation as given by the first harmonic of the heat-flow rate due to the modulation of the sample temperature. A time-dependence of the response to the modulation may be caused by slow, irreversible melting, crystallization, or annealing. A frequency-dependent response of the sample is also linked to thermal resistances causing alternating temperature gradients within the calorimeter. Finally, errors in the reversing signal may be due to a nonlinear and/or nonstationary response [2–4], and, as found with the present samples, due to a shift in baseline, caused by excessive deformation of the sample pan on fiber shrinkage during melting. The term *reversible*, in contrast, is applied in the thermodynamic sense to results which have either been corrected or measured under conditions that are free of the indicated limitations. To measure reversible melting effects, it is usually necessary to apply quasi-isothermal analysis methods by modulation about a constant temperature for extended periods of time to eliminate slow time effects [3,4], although it must be kept in mind that reversible processes also may be slower than the instrument response to the modulation and must then be analyzed at slower frequencies of modulation. The modulation response should be checked in the time domain for symmetry of melting and crystallization, and to prove that there are no instrument or analysis effects [5].

The sample of UHMM-PE analyzed in this paper is a part of the series of UHMM-PE fibers which were studied by differential scanning calorimetry (DSC) [6], temperature-modulated differential scanning calorimetry (TMDSC) based on linear heating and cooling segments [7], atomic force microscopy (AFM) [7], optical microscopy [8,9], full-pattern X-ray diffraction [8], small angle X-ray scattering (SAX) [8], wide-angle X-ray scattering (WAX)

☆ The submitted manuscript has been authored by a contractor of the US Government under the contract no. DOE-AC05-00OR22725. Accordingly, the US Government retains a nonexclusive, royalty-free license to publish, or reproduce the published form of this contribution, or allow others to do so, for US Government purposes.

* Corresponding author.
E-mail address: wunderlich@chartertn.net (B. Wunderlich).

0040-6031/$ – see front matter © 2004 Elsevier B.V. All rights reserved.
doi:10.1016/j.tca.2004.04.003

[10], solid state ^{13}C nuclear magnetic resonance (^{13}C NMR) [11–13], and thermomechanical analysis (TMA) [9]. In the previous research it was revealed that these fibers consist at room temperature of three phases: crystalline, amorphous, and oriented-intermediate. The crystalline phase was about 64% of the fibers and was mainly orthorhombic, with a small amounts of monoclinic crystals [8]. The oriented-intermediate phase could be estimated to be 33%. It is highly strained, with an intermediate mobility between the crystalline and amorphous PE and a heat of fusion of about 43% of that of the orthorhombic crystals [10–15]. The solid state ^{13}C NMR could identify about 3% of truly amorphous polymer [10].

There had been a controversy about multiple melting peaks of UHMM-PE fibers which are frequently observed on DSC analysis. It could be shown, however, that the multiple melting peaks are due to external, longitudinal, or lateral constraints [10]. As soon as the constraints are removed, the high-temperature melting peaks disappear. Bastiaansen and Lemstra [16] reported only one melting peak at 415 K for unconstrained UHMM-PE fibers and Pennings and Zwijnenburg [17] described three or more melting peaks for the same fiber when constrained. Multiple melting peaks of constrained UHMM-PE fibers are also observed by TMDSC with an underlying heating rate [7].

The losses in mechanical properties of UHMM-PE fibers were studied by thermal analysis and atomic force microscopy after annealing at 373 K, below the temperature of major restructuring of the fiber [7]. The molecules of the oriented-intermediate phase, located between the micro- and macro-fibrils seem to slacken on such low-temperature annealing.

In this paper we will discuss the reversing melting and crystallization of the crystalline and metastable crystalline phases of the gel-spun UHMM-PE fibers, using sinusoidally modulated, quasi-isothermal TMDSC. Before this analysis for such samples is possible, it will be shown that a special instrument effect observed on the initial melting of the fibers needs to be identified and eliminated.

2. Experimental

The Thermal Analyst 2920 System™ from TA Instruments, Inc. was used for all TMDSC measurements. Quasi-isothermal TMDSC was done at successive base temperatures, T_0, with sinusoidal modulation. Each run lasted for 20 min with a temperature amplitude of 0.5 K and a period of 60 s. The data of the last 10 min were taken as the result at the investigated temperature, T_0, and plotted as a single point for each measurement. The details of experimentation and mathematical treatment of the quasi-isothermal TMDSC are given in the literature [3,4]. Dry N_2 gas with a flow rate of 25 mL min^{-1} was purged through the DSC cell. Cooling was accomplished with a refrigerated cooling system (RCS, cooling capacity to 220 K). Temperature modulation is controlled at the sample temperature sensing position, underneath the sample calorimeter [3].

The sample temperature was calibrated in the standard DSC mode. The onset-temperature of the transition peak of indium (429.75 K), extrapolated to the baseline, was used for this calibration, using rates of heating of 10 K min^{-1}. The heat-flow rate was calibrated approximately with the heat of fusion of In (28.62 J g^{-1}) [18]. The indium was of the usual, high purity (>99.99%). A single-crystal disk of sapphire (22.5 mg) was the calibrant for the heat-flow rate.

The sample masses were varied from 2.8 down to 0.5 mg, weighed on a Cahn C-33 electro-balance to an accuracy of ±0.001 mg. For all series of experiments the reference pan remained the same. Its mass was slightly smaller than that of the sample pans to allow for easy evaluation of the asymmetry of the calorimeter in TMDSC [19]. Because of the small sample masses, final values of the amplitude were adjusted by shifts parallel to the ordinate to the known heat capacities of the solid fibers below about 350 K [9,10] or of the melt, both known form the ATHAS Data Bank [20].

The samples discussed in this paper are gel-spun fibers of ultrahigh molar mass polyethylene (UHMM-PE). The fibers were provided by Allied-Signal Inc. and had a molar mass of $M_w > 10^6$ Da. They were of the commercial Spectra 900™ type, and are identical to the PE-III fibers, analyzed in Refs. [7–10]. Density, crystallinity, and mechanical properties are summarized in Table 1.

The fibers were cut before placement into the sample pan. Its strands were untwisted and placed between a doubly folded weighing paper. The weighing paper was next taped to a board and cut with a single-edged razor into about 3 mm wide strips. The fibers were then transferred to the DSC pan with the help of the weighting paper. This procedure had the benefit of leaving the fibers largely parallel. The sample was sealed in standard Al pans of 20 μL volume, and laterally compressed with the lid of the pan.

The apparent heat capacities are calculated, as usual, using the results of three runs (a run of an empty pan versus an empty pan to eliminate asymmetry, a second run of an empty pan versus a sapphire-filled pan for the calibration, and finally, the third run of an empty pan versus the sample-filled pan for measurement).

Table 1
Properties of the UHMM-PE fiber III

Sample	Modulus[a] (GPa)	Tensile strength[a] (GPa)	Density[b] (Mg m^{-3})	Crystallinity[b] (%)
PE-III	125	2.7	0.974	86

[a] Data supplied by Allied-Signal Inc.
[b] Data from density, heat capacity and solid state NMR divide the phase structure into ≈3% amorphous, ≈34% oriented-intermediate phase (with a reduced heat of fusion), and ≈63% crystallinity, see Refs. [10,11].

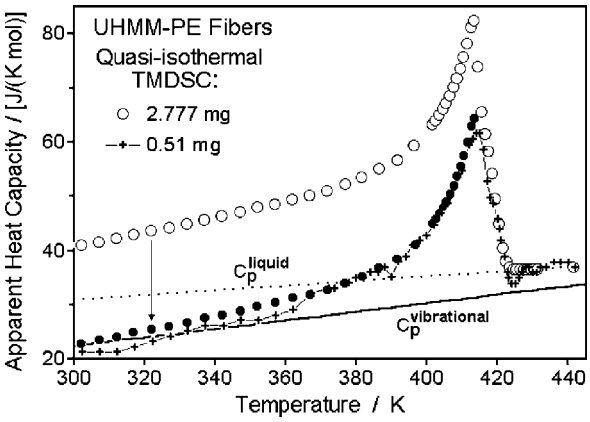

Fig. 1. Apparent, reversing heat capacities of UHMM-PE fibers by quasi-isothermal TMDSC of sample masses of 2.777 and 0.51 mg. Both curves are fitted to the known heat capacity of the liquid state. The filled circles illustrate the fit on an additional, parallel shift of the data of the 2.777 mg sample between 300 and 415 K, as indicated. The dotted and continuous lines are taken from the ATHAS Data Bank for the liquid heat capacity and vibrational heat capacity of the solid, respectively.

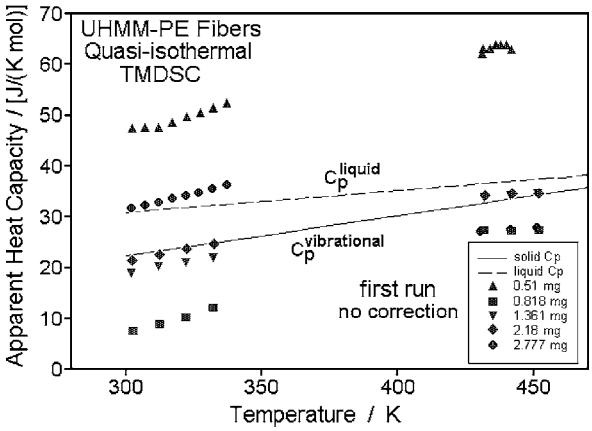

Fig. 2. Uncorrected data on TMDSC of UHMM-PE fiber samples of different masses, taken outside the major melting range on first heating. The sample of 2.777 and 0.51 mg are identical to Fig. 1. The dashed and continuous lines are taken from the ATHAS Data Bank for the liquid heat capacity and vibrational heat capacity of the solid, respectively.

3. Results

The experiments were run with rather low sample masses since it was found earlier that larger masses lead to excessive reorganization to the hexagonal phase due to the lateral constraint of the fibers when closing the pan [6]. On melting, the gel-spun fibers shrink longitudinally and expand laterally causing the multiple melting peaks which accompany the development and ultimate melting of the hexagonal phase [10]. In addition, the rather thin fibers were thought to introduce rather high thermal resistances inside the sample pan. Fig. 1 represents the TMDSC results for 2.777 and 0.51 mg of UHMM-PE gel-spun fibers, measured stepwise, quasi-isothermally, starting from room temperature and going up through the melting region into the pure melt. Both runs were matched to the known heat capacity of the liquid from the ATHAS Data Bank [20] by a shift parallel to the ordinate. The magnitude of the correction can be seen from the raw data, displayed in Fig. 2. A crystallinity of 87% was determined from the heat of fusion measured by standard DSC at 10 K min^{-1} using the orthorhombic heat of fusion, in agreement with the dilatometric density listed in Table 1. The mole in the dimension of the apparent heat capacities refers to a repeating unit of one CH_2-group, i.e., a mass of 14.03 g. The dotted line represents the heat capacity of a 100% amorphous sample extrapolated from the melt to lower temperature, and the solid line is for the vibrational heat capacity of a 100%-crystalline sample, as given in the ATHAS Data Bank [20]. The apparent heat capacity of the 2.777 mg sample below the melting peak appears to be higher than expected by about 18 J K^{-1} mol^{-1}. The low-mass sample gives a more reasonable answer. The end of melting is seen at 426 K, considerably above the equilibrium melting temperature of 414.6 K [21].

Additional measurements were made to investigate this high apparent heat capacity of the original fibers below the melting peak. Samples of similar mass were prepared in different manners, for example, by not cutting fibers, winding them around a small rod, or packing them into a pan with aluminum oxide powder to improve the thermal conductivity throughout the DSC pan. All showed various levels of excessively high heat capacities before melting when fitted to what was thought to be the heat capacity of the equilibrium melt. Standard DSC runs of the same samples showed the expected, larger melting peak, accounting for the additional nonreversing melting. Melting peaks of about 400 J K^{-1} mol^{-1} are seen, but have reached for a small, unrestrained mass of 24 μg a very narrow peak of over 1000 J K^{-1} mol^{-1} [6,9]. It was furthermore noted, that up to the beginning of melting all higher data in the initial quasi-isothermal runs could be corrected by a parallel shift as indicated in Fig. 1 for the 2.777 mg sample.

To gain more information, a systematic check of different masses was made at temperatures before melting and in the subsequently reached melt. Fig. 2 shows the results of five of these series, but before any fitting of the data by shifts parallel to the ordinate. As expected, there is a reasonable scatter of the heat capacities because of the rather low masses analyzed. All data in the low-temperature region could be brought to coincidence by parallel shifting at the low-temperature to the expected heat capacity of an 87%-crystalline sample, but then the liquid heat capacities would be incorrect, as can be seen for one of the samples in Fig. 5. Similarly, by shifting of the heat capacity data parallel to the ordinate of the melt to the expected values, the data at low temperature are unacceptable.

Fig. 3 indicates that at low temperature, the quasi-isothermal data of the 0.51 mg sample compare reasonably well

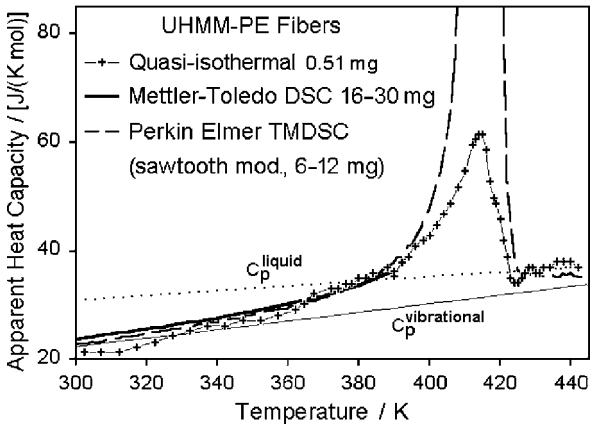

Fig. 3. Apparent, reversing heat capacities of 0.51 mg UHMM-PE by quasi-isothermal TMDSC (thin line with pluses, this research). Comparison to previous data of Ref. [10] which reach up to 390 K (solid line, see also Fig. 7) and Ref. [7] (dashed line, see also Fig. 8). The dotted and continuous lines are taken from the ATHAS Data Bank for the liquid heat capacity and vibrational heat capacity of the solid, respectively.

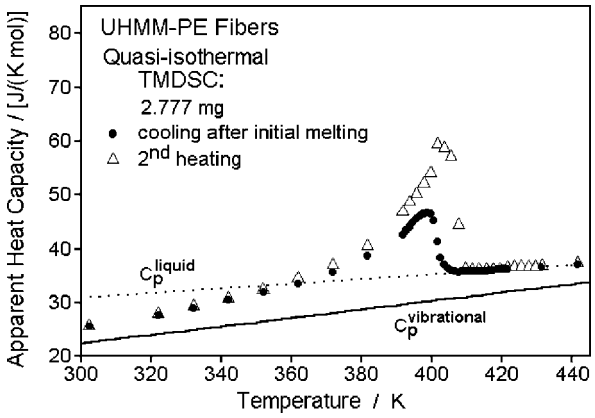

Fig. 4. Apparent, reversing heat capacities of UHMM-PE by quasi-isothermal TMDSC of sample mass 2.777 mg from Fig. 1 measured after melting on cooling and on subsequent second heating. Both curves are fitted to the known heat capacity of the liquid state. The dotted and continuous lines are taken from the ATHAS Data Bank for the liquid heat capacity and vibrational heat capacity of the solid, respectively.

to the prior precision measurements by modified standard DSC on 30–60 times heavier samples of the same batch of fibers [10]. These latter experiments were done in small, 20 K steps, interrupted with isotherms to reestablish the baseline. The heating sequences were stopped before major melting occurred and followed by analogous measurements on cooling and repeated. The overall accuracy was estimated to be about 1.0%, the heat-flux calorimeter was of the Mettler DSC820 type (see also Fig. 7). It was found later, that another reason for the good precision of these data was that the measurements were made in the much bigger, more sturdy pans supplied by Mettler-Toledo (≈50 mg). A further comparison, again from the same batch of fibers, is shown by the broken line in Fig. 3 [7] (see also the data represented by +++ in Fig. 8). This curve was obtained from a saw-tooth-modulated run with sufficiently long periods, so that each heating cycle could be analyzed as a standard DSC segment in steady state [22]. The calorimeter was of the power-compensation type (Perkin Elmer, Pyris-1). Below 395 K all three measurements agree.

After the initial melting, shown in Fig. 1, the analysis of the 2.777 mg sample was continued without interruption as documented in Fig. 4. First, measurements were done quasi-isothermally on cooling from the melt, showing the effect of crystallization and, then, after reaching low temperatures, continued on reheating to melt the crystals grown during the cooling run. The results in Fig. 4 were fitted to the ATHAS Data Bank in the initial temperature region of the melt. In these later stages of the run, the data are reproducible and as expected from prior experimentation. Another series of quasi-isothermal runs on cooling after the second heating was performed, but is not depicted, since it was identical to the cooling sequence shown in Fig. 4.

4. Discussions

The first result to be discussed is the excess apparent reversing heat capacity seen in Fig. 1 from room temperature to the beginning of the melting peak which varied irreproducibly with sample masses as seen in Fig. 2 and also with sample preparation. The excess reversing heat capacity of the 2.777 mg sample could not be caused by thermal lags or sluggish latent heat processes within the sample since both of these would retard the heat-flow and yield a lower heat capacity than expected. The quasi-isothermal method of TMDSC was developed to study and eliminate slow, time-dependent processes within the sample [3,4]. The time-dependent processes that have been studied in this fashion are the glass transitions, where the cooperative, conformational motion of macromolecules reaches the time scale of the modulation [23], and the latent heat effects which are involved in phase transitions such as melting, crystallization, annealing and recrystallization [1]. The glass transition of the analyzed fibers is known to be completed at about 300 K [9,10] (see also Fig. 7). Irreversible latent heat effects could not cause the excess heat capacity in Fig. 1 either, since no significant decrease with time was observed in the quasi-isothermal measurements. Truly reversible phase transitions are also not possible since they would also have to show in the total heat capacity of the standard DSC in Fig. 3, which they do not.

In Fig. 5, a comparison of the raw data is given for the 2.777 mg, initial melting run, together with the attempt to first, match the raw data at low temperature to the expected vibrational heat capacity, and then, match, as also done for Fig. 1, in the melt to the ATHAS Data Bank. Clearly, if both matches to the known results are to hold, something must have happened at the reversing melting peak, as marked in the figure at 415 K for the three data sets. The solution to the problem was found when inspecting the sample pans before

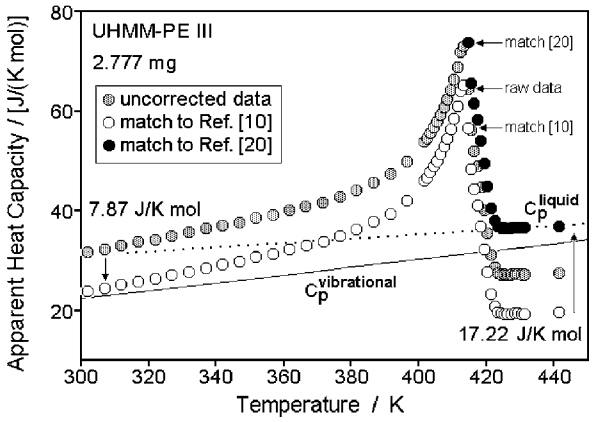

Fig. 5. Apparent, reversing heat capacities of UHMM-PE fibers by quasi-isothermal TMDSC of sample masses of 2.777 mg as in Fig. 1. Uncorrected data and attempted fittings to the known heat capacity of the low-temperature solid state and the high-temperature liquid state. The dotted and continuous lines are taken from the ATHAS Data Bank for the liquid heat capacity and vibrational heat capacity of the solid, respectively.

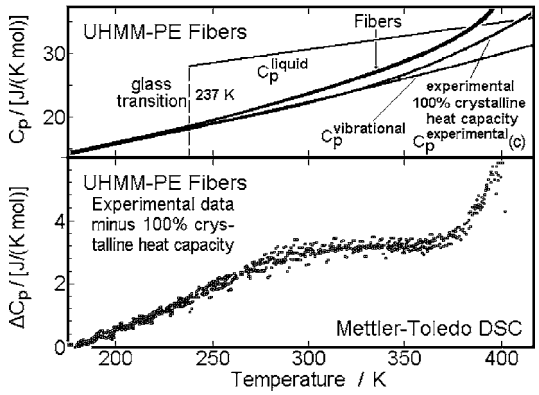

Fig. 7. Heat capacity of gel-spun UHMM-PE fibers [9,10]. Standard scans of successive 20 K steps over the indicated temperature range, interrupted with 1.0 min isotherms, followed by an analogous cooling run and repeat measurements (Mettler-Toledo DSC 820, 16–30 mg of sample). The top graph contains the averaged experimental data, compared to data-bank information [20]. The bottom graph is a plot of the difference between the C_p of the fibers and C_p of 100%-crystalline PE [20], shown with an expanded ordinate. The figure is redrawn from Ref. [10], to correspond to the present sample.

and after the run. As shown on the left in Fig. 6, the pan bottom is flat for the unused pan. The 0.51 mg sample underwent some deformation on melting, the 2.777 mg sample shows the largest deformation on melting due to the shrinking of the fibers and the resulting expansion in diameter. These changes in the pan shapes cause shifts in the baseline, negating calibrations at the low temperature for higher temperatures and vice versa. This shift of baseline due to pan deformation will be discussed elsewhere in more detail, based on frequency-dependent TMDSC [24]. It is not only of importance to the analysis of fibers which undergo extreme shrinkage, but can also be observed for polymer melts which wet the Al surface and dislocate the sample into the closure seam and then, on cooling to the solid state, can deform soft aluminum pans.

Only after the problem of deformation of the sample pan during melting could be resolved, was it possible to tackle the discussion of the reversible and reversing heat capacities of the UHMM-PE gel-spun fibers in the various temperature ranges. Up to about 390 K, the heat capacities of Fig. 3 by standard DSC [10], TMDSC with an underlying heating rate [7], and the new quasi-isothermal C_p agree, but show a reversible excess heat capacity relative to the

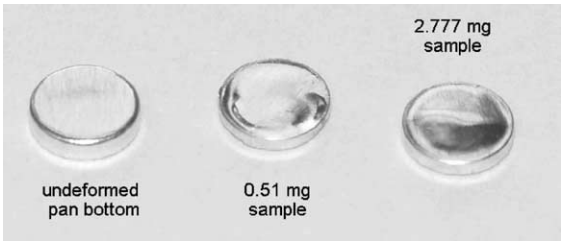

Fig. 6. Photograph of the bottoms of a new aluminum DSC pan (left) and the 0.51 and 2.777 mg samples after completion of the runs in Figs. 1 and 4.

known vibrational heat capacity of polyethylene [20]. The conclusion that this excess heat capacity is reversible is based on the equality of the three measuring methods. Measurements on heating and cooling are identical and equal to the standard DSC measurements. Furthermore, extended runs in the quasi-isothermal mode do not show noticeable changes with time. Fig. 7 shows the analysis of the data using the interpretation given in [10]. At about 300 K, the glass transition of the fibers is complete, and up to about 360 K the heat capacity stays about 2.6 $J\,K^{-1}\,mol^{-1}$ above that of the experimental, 100%-crystalline polyethylene, as expected for a semicrystalline sample. The increase from the vibrational heat capacity to the experimental, 100%-crystalline heat capacity is due to the well-known *trans-gauche* interchanges in the crystal [10]. Above 360 K, the difference of the heat capacities of the fibers relative to the 100%-crystalline polyethylene starts to increase.

Fig. 3 shows that above 360 K the C_p by quasi-isothermal analysis increases less rapidly than the C_p by TMDSC with an underlying heating rate. The difference between the two experiments indicates the irreversible latent heat effect consisting of a slow reorganization of the crystal structure. The difference between the quasi-isothermal C_p and the vibrational C_p, or better the experimental C_p of 100%-crystalline polyethylene corrected for the amorphous and mesophase material is a measure of the reversible latent heat contribution. Quasi-isothermal TMDSC was earlier performed with saw-tooth modulation [7] which can be analyzed using only data after each heating or cooling step has reached steady state [22]. Both quasi-isothermal measurements yielded comparable results, as can be seen by comparing Figs. 3 and 8. The peak heights of both first run experiments were close to 60 $J\,K^{-1}\,mol^{-1}$ at a temperature of about 410 K.

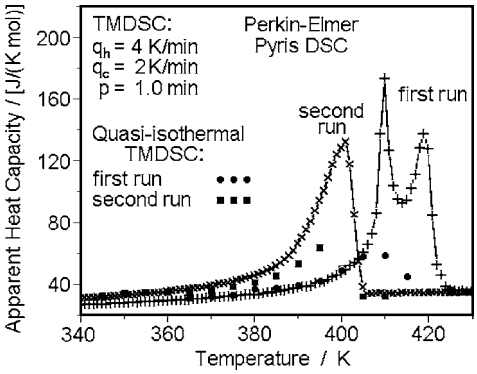

Fig. 8. Saw-tooth-modulated TMDSC of gel-spun UHMM-PE fibers (6–12 mg), analyzed with standard DSC-based technique [22] (heating rate: 4.0 K min^{-1}, cooling rate: 2.0 K min^{-1}, underlying heating rate: 1.0 K min^{-1}, period: 1.0 min, data marked by + and ×). The quasi-isothermal data points were generated after 10–130 min of modulation at the given temperature, dependent on the time needed to reach steady state (heating rate and cooling rates are 2.0 K min^{-1}, period: 1.0 min). The figure is redrawn from Ref. [7].

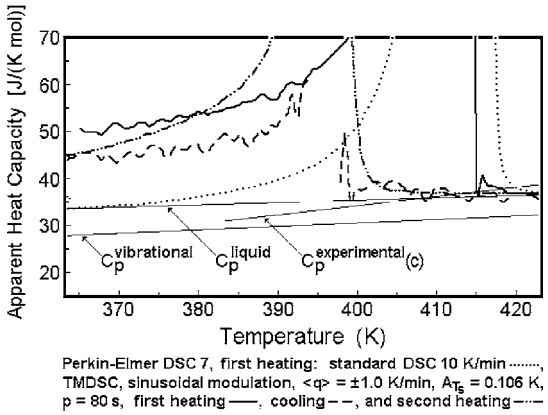

Fig. 9. Thermal analysis results on 0.7 mg of nascent UHMM-PE, redrawn after data from [27].

On recrystallization by cooling from the melt, the peak in Fig. 4 reaches only 45 J K^{-1} mol^{-1}, but increases to its previous level on the second run at 10 K below the peak of the first run. The TMDSC with an underlying heating rate in Fig. 8 show much higher reversing melting peaks. The double-peak on first melting indicates reorganization to the hexagonal, metastable crystal structure based on the residual strain in the fibers, discussed in detail in Refs. [7,10]. The quasi-isothermal TMDSC in Fig. 3 reveals only a weak high-temperature shoulder which may be an indication of some orthorhombic-to-hexagonal crystal transition in the lower temperature of the melting range.

The end of melting depends also strongly on the measuring method. The equilibrium melting temperature of high-molar-mass polyethylene is 414.6 K [21]. The standard DSC of the UHMM-PE fibers at a heating rate of 0.1 K min^{-1} leads to a melt end of about 428 K, which on raising the heating rate to 10 K min^{-1} moves to 438 K [8], a clear sign of superheating. Both TMDSC runs in Fig. 3 show melting ends of about 426 K. Only on the second melting in Fig. 4 is the melting end at 412 K, which is below the equilibrium melting temperature, and possibly free of superheating. The onset of crystallization of 408 K is somewhat lower in temperature than the usual supercooling of polyethylene of about 6–10 K [1]. Since the crystals of the gel-spun fibers are known to be small [8], superheating is not an effect of the crystal size, but of remaining strain in the melt attached to the crystal. This strain can cause melt orientation and a reduction of the entropy of melting which temporarily increases the melting temperature until the strain dissipates with the melting of the crystals ($T_m = \Delta H_f / \Delta S_f$).

The final part of the discussion contains a comparison of the thermal analysis of the gel-spun UHMM-PE with UHMM-PE of different crystallization histories and other polyethylenes [1]. The TMDSC with an underlying heating rate on nascent UHMM-PE reveals a similar excess heat capacity before the first melting [25,26]. The nascent UHMM-PE is crystallized shortly after polymerization and may not have reached the structure of the random melt before crystallization. In this case the crystal structure may be also fibrillar, as discussed in more detail, for example in Ref. [27]. The conditions of these measurements and the results are redrawn in Fig. 9 to match the units of this discussion. The excess heat capacity beyond that of the values by standard DSC at about 360 K is similar to the UHMM-PE gel-spun fibers in Fig. 1. Despite some similarity, this material behaves differently. On increasing the modulation frequency, the excess in heat capacity below 300 K decreases to the level of the standard DSC. The nascent UHMM-PE has, thus, in this low-temperature region an irreversible change in structure, as suggested in [26], which is not seen in the gel-spun fibers. On cooling and second heating, furthermore, the crystallization and melting peaks are shifted to lower temperature, but the decrease in the low-temperature, reversing heat capacity does not reach the level set by the standard DSC trace seen in Fig. 1. At higher temperatures, qualitatively similar reversing and reversible processes have been observed with the nascent UHMM-PE, but with somewhat smaller superheating. Model calculation of the frequency dependence of the reversing C_p allowed speculations about different irreversible and reversible processes in this temperature range [25,26].

On gel-crystallization from solution, the sample of the UHMM-PE of Fig. 5 was observed to have a lamellar, folded-chain crystal morphology with 13 nm thick crystals. Again, the reversing heat capacity exceeded the total heat capacity and its reversing heat-flow rate was a substantial part of the total heat-flow rate [28]. In the region of the large reversing heat-flow rate, the fold-length was observed to increase by a factor of two, so that melting and recrystallization may contribute to the reversing effect. Stretching the gel-crystallize sample below the melting temperature

leads to similar changes as observed here and shown earlier also in Ref. [28].

5. Conclusions

The resolution of the change of baseline on melting of polymers due to deformation of the sample pan was a problem that delayed the discussion of the TMDSC data on gel-spun fibers for about 2 years. It is an effect that should be checked for whenever samples expand during measurement or can wet the pan material and grossly change the calorimeter geometry defined by pan and sample. Further work on this topic of importance to the quantitative DSC is in progress [24].

The reversible heat capacity in the melting range of the gel-spun UHMM-PE is contrasting the behavior of extended-chain crystals of polyethylene which have practically no reversible heat capacity contributions in the melting range [29]. Linear polyethylene with average molar mass and mainly chain-folded structure also exhibits less reversible melting. Comparison of several analyses suggests a peak of about $40\,J\,K^{-1}\,mol^{-1}$ [1]. This reversible melting is caused by melting and crystallization on the lateral crystal surfaces by decoupled chain segments of the polymer [30] and also linked to the earlier observed reversible changes in crystal thickness of chain-folded polyethylene [31]. They also are not comparable to the gel-spun UHMM-PE fibers because of their different crystal morphology. This spectrum of data shows that thermal analysis is the most useful technique of identifying various polymer morphologies. Since the gel-spun fibers have little regular chain folds, one must suggest that the local, reversible melting observed by the quasi-isothermal TMDSC originates from melting and crystallization of ordered, decoupled chain segments of orthorhombic or mesophase regions. Similar indication of reversible melting of such local, fringed micellar-like structures are seen in low-molar-mass polyethylenes [29,32] and linear-low-density polyethylene [33].

Although the earlier data on gel-spun polyethylene are only qualitative [28], they allow a link of the thermal analysis from the first, nascent structure to the gel-crystallized lamellae, and furthermore to the gel-spun fibers, and ultimately to the second runs of the melt-crystallized, bulk materials. Further links to lower molar mass polyethylenes, its copolymers, and oligomers are given in Ref. [1] and make polyethylene one of the best studied polymer and point to the conclusion that more quantitative thermal analyses, coupled with phase-structure and mobility studies allow a detailed description of such multi-phase polymers.

Acknowledgements

This work was supported by the Division of Materials Research, National Science Foundation, Polymers Program, Grant No. DMR-0312233 and the Division of Materials Sciences, Office of Basic Energy Sciences, US Department of Energy at Oak Ridge National Laboratory, managed and operated by UT-Battelle, LLC, for the US Department of Energy, under contract number DOE-AC05-00OR22725.

References

[1] B. Wunderlich, Prog. Polym. Sci. 28 (2003) 383.
[2] M. Merzlyakov, C. Schick, Thermochim. Acta 330 (1999) 330.
[3] A. Boller, Y. Jin, B. Wunderlich, J. Thermal Anal. 42 (1994) 307.
[4] B. Wunderlich, Y. Jin, A. Boller, Thermochim. Acta 238 (1994) 277.
[5] C. Schick, M. Merzlyakov, B. Wunderlich, Polym. Bull. 40 (1998) 297.
[6] A. Boller, B. Wunderlich, J. Thermal Anal. 49 (1997) 343.
[7] W. Hu, A. Buzin, J.-S. Lin, B. Wunderlich, J. Polym. Sci. Part B: Polym. Phys. 41 (2003) 403.
[8] Y. Fu, W. Chen, M. Pyda, D. Londono, B. Annis, A. Boller, A. Habenschuss, J. Cheng, B. Wunderlich, J. Macromol. Sci.: Phys. B35 (1996) 37.
[9] A. Boller, Thesis, University of Tennessee, Knoxville, 1996.
[10] Y.K. Kwon, A. Boller, M. Pyda, B. Wunderlich, Polymer 41 (2000) 6237.
[11] W. Chen, Y. Fu, B. Wunderlich, J. Cheng, J. Polym. Sci. Part B: Polym. Phys. 32 (1994) 2661.
[12] J. Cheng, M. Fone, Y. Fu, W. Chen, J. Thermal Anal. 47 (1996) 673.
[13] J. Cheng, M. Fone, V.N. Reddy, K.B. Schwartz, H.P. Fisher, B. Wunderlich, J. Polym. Sci. Part B: Polym. Phys. 32 (1994) 2683.
[14] K. Kaji, Y. Ohta, H. Yasuda, M. Murano, Polym. J. 22 (1990) 455.
[15] K. Kaji, Y. Ohta, H. Yasuda, M. Murano, Polym. J. 22 (1990) 893.
[16] C.W.M. Bastiaansen, P.J. Lemstra, Makromol. Chem. Makromol. Symp. 28 (1989) 73.
[17] A.J. Pennings, A. Zwijnenburg, J. Polym. Sci. Part B: Polym. Phys. 17 (1979) 1011.
[18] S.M. Sarge, E. Gmelin, G.W.H. Höhne, H.K. Cammenga, W. Hemminger, W. Eysel, Thermochim. Acta 247 (1994) 129.
[19] K. Ishikiriyama, B. Wunderlich, J. Thermal Anal. 50 (1997) 337.
[20] B. Wunderlich, The ATHAS Data Base on heat capacities of polymers, Pure Appl. Chem. 67 (1995) 1919. For data see the internet address: http://web.utk.edu/~athas/databank;
B. Wunderlich, Heat capacity of polymers, in: S.Z.D. Cheng (Ed.), Handbook of Thermal Analysis and Calorimetry, Applications to Polymers and Plastics, Elsevier, Amsterdam, vol. 3, 2002, pp. 1–47.
[21] B. Wunderlich, G. Czornyj, Macromolecules 10 (1977) 906.
[22] W. Hu, B. Wunderlich, J. Thermal Anal. Calorimetry 66 (2001) 677.
[23] B. Wunderlich, A. Boller, I. Okazaki, S. Kreitmeier, J. Thermal Anal. 47 (1966) 1013.
[24] M. Pyda, E. Nowak-Pyda, J. Pak, B. Wunderlich, in press.
[25] G.W.H. Höhne, L. Kurelec, Thermochim. Acta 377 (2001) 141.
[26] G.W.H. Höhne, L. Kurelec, S. Rastogi, P.J. Lemstra, Thermochim. Acta 396 (2003) 97.
[27] B. Wunderlich, Macromolecular physics, in: Crystallization During Polymerization, vol. II, Section 6.4, Academic Press, New York, 1976, pp. 271–347.
[28] G.W.H. Höhne, Thermochim. Acta 330 (1999) 93.
[29] J. Pak, B. Wunderlich, J. Polym. Sci. Part B: Polym. Phys. 40 (2002) 2219.
[30] R. Androsch, B. Wunderlich, J. Polym. Sci. Part B: Polym. Phys. 41 (2003) 2157.
[31] B. Goderis, H. Reynaers, R. Scherrenberg, V.B.F. Mathot, M.H.J. Koch, Macromolecules 34 (2001) 1779.
[32] J. Pak, B. Wunderlich, Macromolecules 34 (2001) 4492.
[33] R. Androsch, B. Wunderlich, Macromolecules 33 (2000) 9076.